Applied Catalysis B: Environmental 312 (2022) 121382

Contents lists available at ScienceDirect

Applied Catalysis B: Environmental

journal homepage: www.elsevier.com/locate/apcatb

# Unraveling the Mo/HZSM-5 reduction pre-treatment effect on methane dehydroaromatization reaction

Ángeles López-Martín, Alfonso Caballero, Gerardo Colón *

*Instituto de Ciencia de Materiales de Sevilla, Centro Mixto Universidad de Sevilla-CSIC, Américo Vespucio s/n, 41092 Sevilla, Spain*

ARTICLE INFO

*Keywords:*
Molybdenum
ZSM-5
Pre-treatment
Methane
Dehydroaromatization

ABSTRACT

Reduction pre-treatment at different temperatures were performed over Mo/HZSM-5 system before methane dehydroaromatiztion reaction. We have shown the crucial effect of reduction temperature on the final catalytic performance. Outstanding improvement in the aromatics conversion has been attained. Thus, $H_2$ formation form methane cracking reaction seems to be hindered for pre-treated catalysts. As a consequence, the deposition of coke in these samples appeared also notably suppressed. The optimum performance has been achieved for reduction pre-treatment at 550 ºC. For this temperature, we have observed that the fraction of reduced Mo species is higher.

## 1. Introduction

Natural gas, mainly composed of methane, is a promising alternative carbon source, competing to replace the use of petroleum in the industry [1,2]. For this reason, last progresses in the production technology of natural gas have lowered prices for methane. Therefore, the interest in converting methane to higher value products has become renewed [4,5]. Methane is a very abundant and widely distributed around the globe fossil fuel resource. However, because of its high C−H bond energy, methane molecule is difficult to activate so is currently used mostly as an energy source. On the contrary, two different routes have been proposed for utilizing methane to valuable products, that is indirect and direct conversion processes [5,6]. Within indirect conversion, methane is converted into syngas and then, through a Fischer–Tropsch process, into other hydrocarbons. Such multi-step process results in a high energy consumption. In contrast, direct conversion shows both energetic and economic advantages [7]. Non-oxidative direct reaction has been pointed as the more appropriate approach to increase the selectivity to specific desired product [8,9]. Methane dehydroaromatization (*MDA*) is considered one of the most attractive among the alternative reactions [10,11]. Value-added chemicals, such as benzene, toluene and xylene, obtained as products, can be used as industrial feedstock chemicals [3,12]. However, *MDA* is an extremely thermodynamically unfavorable reaction, limited to ca. 13% yield to benzene at typical reaction conditions [13,14]. Moreover, the side formation of solid carbon and hydrogen from methane cracking is a serious disadvantage which leads to catalyst deactivation [3,15]. Under non-oxidative conditions, *MDA* reaction can be achieved using zeolites and oxide-based catalysts at elevated temperatures [16,17].

As above anticipated, at such temperatures at which the reaction produces interesting yields of benzene (i.e. between 650 and 800 °C), coke formation radically leads to the fast deactivation of the catalysts [18,19].

Till now, due to its outstanding performance reported, catalysts based on Mo supported on different zeolites remains by far the most studied for *MDA* reaction [20]. In order to improve the *MDA* activity of Mo/HZSM-5, as well as to inhibit deactivation, various approaches, such as promoter addition and pre-treatment, have been undertaken.

Although the literature results appear controversial, improving effects have been reported using different metals as promoters [21–26].

On the other side, in spite of the interesting performance showed by Mo-based systems, the dramatic deactivation usually reported seriously hinders the industrial transfer of this process [13,27,28]. Many studies have pursued to elucidate the origin of the drastic deactivation observed in Mo/HZSM-5 catalysts during the *MDA* reaction. Thus, it has been argued that extensive formation of polyaromatic hydrocarbon carbon deposits is the main reason for catalyst deactivation [29].

In this sense, Tempelman et al. reported that the effect of pre-reduction of Mo/HZSM-5 at 700 ºC under inert (He), oxidizing (artificial air), or carburizing ($CH_4$/He mixture) atmospheres [30]. Thus, they pointed out that precarburization in methane gave catalysts showing high aromatic selectivities as well as low deactivation rates. They

* Corresponding author.
*E-mail address:* gcolon@icmse.csic.es (G. Colón).

https://doi.org/10.1016/j.apcatb.2022.121382
Received 16 February 2022; Received in revised form 17 March 2022; Accepted 5 April 2022
Available online 14 April 2022

pointed out that the rapid formation of molybdenum carbides during pre-treatment hinders the amount of mobile molybdenum oxide species and so, their diffusion into the micropores. In this line, Portilla et al. showed that the optimum Mo speciation was achieved by pre-treatment at increasing temperature under $N_2$ flow [31,32].

Indeed, different catalyst pre-treatment has been reported pursuing to extend the life and stability of the catalyst [22,33]· In all cases, the reduction pre-treatment was performed at reaction temperature and led to a certain catalyst stabilization. The reason of such improvement seems to be correlated to the early formation of Mo-carbide species and the higher dispersion on the support. As a general remark, the formation of metallic Mo at lower temperature was always associated to better catalytic performance. Moreover, though Mo carbides present in the spent catalysts is the same for samples treated by pre-reduction, the Mo carbide particles are smaller.

In this sense, *ex-situ* previous formation of Mo-carbide showed better catalytic performance, denoting that by separation of active site pre-conditioning and reaction processes would improve the catalyst reaction [34].

In this paper, we study the effect of pre-reduction treatment at different temperatures under $H_2$ flow on the final catalytic performance of 4%Mo/HZSM-5 on *MDA* reaction. We discuss in depth how the different reduction temperature would be crucial and strongly affects to the catalyst structural, chemical and morphological features that drastically conditions the final performance.

## 2. Experimental

### 2.1. Catalyst preparation

Commercial ZSM-5 (Si/Al=23, Alfa Aesar) was used as the support for the catalysts. In order to obtain its protonated form, commercial ZSM-5 was initially calcined at 550 °C for 3 h. Then, molybdenum was supported on the zeolite by means of impregnation method [35]. As Mo metal-precursor, ammonium heptamolybdate tetrahydrate ($(NH_4)_6Mo_7O_{24}.4H_2O$ Sigma Aldrich) was used. ZSM-5 support was suspended in water-Mo solution with the stoichiometric amounts of precursor (to achieve metal loading of 4 wt%) and stirred for 20 h. After that, water was eliminated in a rotary evaporator, and the resulting sample was dried at 120 °C for 12 h. Finally, the obtained powder was calcined at 550 °C at 5 °C/min for 3 h. From ICP-OES analysis of the sample, Mo content in the catalyst is 4.1 wt%. The as-prepared catalysts were named as 4%Mo/HZSM-5.

### 2.2. Catalytic activity

The catalytic studies were performed in a stainless-steel tube fixed-bed reactor with 0.1 g of different catalysts diluted in 0.1 g of SiC located between two quartz wool plugs. *MDA* reaction was performed under $CH_4/N_2$ flow (85% in methane) at 5 mL/min, from 50 ºC to at 700 °C using a temperature ramp of 10 °C/min. Reaction products were analyzed by using online GC (Agilent, 7890B) equipped with 3 channels for separate analyses of light gases (MolSieve 5A column, HAYESEP Q precolumn, thermal conductivity detector, TCD), light hydrocarbons (GS-GASPRO column, flame ionization detector, FID) and aromatics (HP-88, flame ionization detector, FID). For the sake of reproducibility, all catalytic experiments were performed twice.

Alternatively, pre-reduction treatment at different temperatures were performed before reaction. For reduction treatment, pure $H_2$ was flown at 25 mL/min for one hour at temperatures between 450 ºC and 650 ºC (at temperature ramp 10 ºC/min). After which, the temperature was lowered to 150 ºC and the flow changed to $CH_4/N_2$ (Scheme 1).

The methane conversion ($X_{CH_4}$) and benzene/aromatics selectivity ($S_{C_6H_6}$, $S_{aromatics}$) were calculated using Eqs. 1 to 3.

$$X_{CH_4} = \frac{[CH_4]_t}{[CH_4]_i} \times 100 \quad (1)$$

$$S_{C_6H_6}(\%) = \frac{[C_6H_6]_t \times 6}{\sum [product_i]_t \times n_i} \times 100 \quad (2)$$

$$S_{aromatics}(\%) = \frac{[aromatics]_t \times 6}{\sum [product_i]_t \times n_i} \times 100 \quad (3)$$

### 2.3. Catalyst characterization

BET surface area measurements were carried out by $N_2$ adsorption at − 196 ºC using a Micromeritics Tristar instrument.

XRD patterns of the studied catalysts were obtained by using a Siemens D-501 diffractometer with Ni filter and graphite monochromator and using the Cu $K_\alpha$ radiation.

The amount of coke deposited after reaction was analyzed by a TA Instruments Q600 TGA/DSC instrument. For this purpose, sample was placed in an alumina crucible and heated to 800 ºC under air flow.

The transmission electron microscopy (TEM) images, high angle annular dark field (HAADF) and element mapping analysis images were obtained on the equipment FEI S/TEM Talos F200S. Samples were prepared by dipping a carbon grid in to the powder sample.

TPR and TPD analysis were carried out using a Quantachrome Chemstar instrument equipped with a thermal conductivity detector and mass spectrometer. About 35 mg of catalyst was first heated to 150 °C in an inert flow of argon at 30 mL/min for 60 min previous to each experiment.

XPS data were recorded on pellets which were outgassed in the prechamber of the instrument at room temperature up to a pressure below $2{\cdot}10^{-8}$ torr to remove chemisorbed water from their surfaces. *In-*

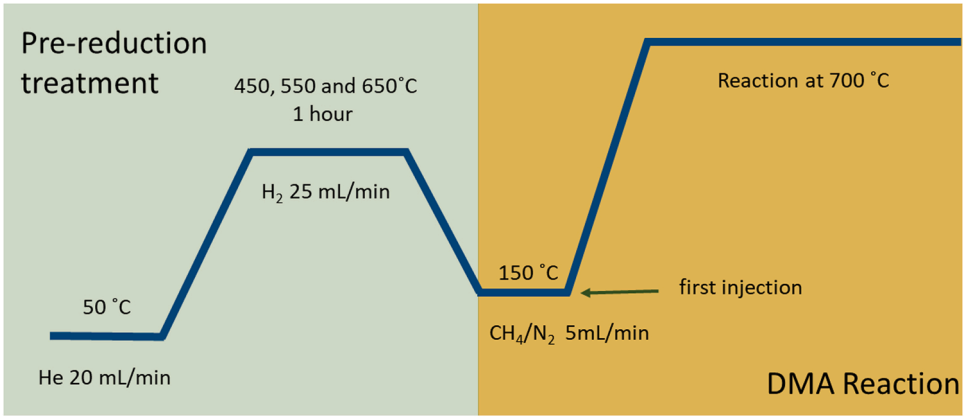


**Scheme 1.** Pre-treatment and reaction scheme followed in this study.

*situ* thermal treatments were accomplished in a cell directly attached to the main chamber, allowing treatment while in contact with a mixture of gases emulating the TPR experiments. Transfer to the main chamber were accomplished under vacuum conditions, where spectra were recorded using a VG Scalab 210 spectrometer, working with constant pass energy of 50 eV. The spectrometer main chamber, working at a pressure below $2{\cdot}10^{-9}$ torr, is equipped with a Specs Phoibos 100 hemispherical electron analyser with a dual X-ray source working with Mg Kα (hν= 1254 eV) at 120 W and 30 mA. Si *2p* signal (103 eV) was used as internal energy reference in all the experiments.

## 3. Results and discussion

### 3.1. Methane dehydroaromatization (MDA) performance

The first important issue to highlight is that the effect of reduction treatment on the catalytic performance strongly depends on the temperature. Obtained initial methane conversions laid in all cases around 10–12%, which is in accordance to reported thermodynamic equilibrium conversion of methane in this reaction [36]. Thus, by observing the evolution of conversion values, we evidenced that pre-reduction treatments seem to affect negatively with respect to not pre-treated sample (Fig. S1). This is due to the contribution of methane cracking in that later sample that would enhance methane conversion in the overall process. Therefore, in order to avoid the important contribution of methane cracking reaction in the methane conversion, we show the conversion to aromatics (Fig. 1). As we can observe, while reduction at 450 ºC surprisingly leads to a noteworthy detrimental effect, the reduction at 550 ºC clearly induces an outstanding improvement. The higher reduction temperature at 650 ºC does not infer any enhancement with respect to non-pre-treated catalyst. Thus, considering that previous results in the literature only refers the reduction pre-treatment at reaction temperature, that is at 700 ºC, our results appear quite interesting in order to optimize the catalyst performance.

In Fig. 2 we show the yields to different aromatic products (benzene, naphthalene, and toluene). In all cases, the higher yields are attained for pre-reduction treatment at 550 ºC. Moreover, it can be noticed that pre-reduction at 450 ºC clearly favors the formation of benzene at the expense of naphthalene. In particular, the selectivity to benzene is more stable for 550 ºC pre-treated catalyst, with values between 62% and 56% of selectivity to $C_6H_6$ during the reaction (Fig. S1).

On the contrary, it is worthy to note the slightly higher formation of naphthalene upon reaction after 550 ºC and 650 ºC reduction treatment (Fig. 2). So, larger conversion to aromatics and greater selectivity is clearly observed in the case of the sample reduced to 550 ºC.

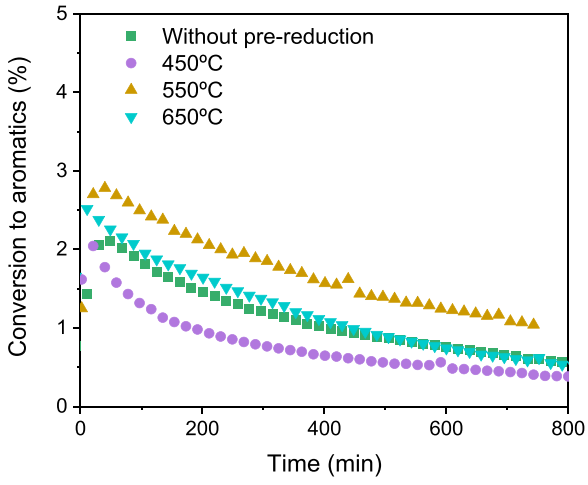


**Fig. 1.** Aromatics conversion plot for 4%Mo/HZSM-5 catalysts during methane dehydroaromatization reaction.

As it has been widely reported, $H_2$ and coke formation from methane cracking is an undesirable process that would compete with methane aromatization [37]. Thus, the observation of $H_2$ production would serve not only as an indication of the dehydrogenation process but also of cracking and therefore catalyst deactivation by coke formation.

Upon these considerations, we may notice that the higher $H_2$ production is observed for the non-pre-treated catalyst (Fig. 3**.a**). For all pre-reduced catalysts, the $H_2$ evolved is notably lower. As a general trend, the total conversion of methane (Fig. S1) reaches its maximum at the beginning of the reaction, obtaining values of ca. 16% in non pre-treated 4%Mo/HZSM-5 and slightly smaller conversion values for the pre-treated catalysts. This fact can be understood by considering the lower methane consumption to form coke and hydrogen.

In this sense, pre-reduction treatment clearly conditions the $H_2$ evolution at the first stage of the reaction pointing out the different reaction pathway during the carbide formation (Fig. 3**.b**). It is widely accepted that within the reaction induction period, Mo oxide species are firstly reduced and then carburized to Mo carbide species when exposed to the $CH_4$ reactant [38,39,43].

Such new Mo-species are proposed to be responsible for activating $CH_4$, and the initial C-C bond formation to $C_2$ species. In the case of pre-reduced catalysts methane would proceed directly to the carburization step leading to a lower $H_2$ evolution.

Additionally, a lower $H_2$ formation would also indicate a lower contribution of coke formation reaction in the overall methane conversion. Indeed, DTG results obtained for the spent 4%Mo/HZSM-5 with and without pre-treatment (Fig. S2) confirmed that the amount of coke formed during the different stages are similar for the pre-treated samples, being much smaller than the amount obtained for the sample without pre-treatment. Thus, we could state that heating the catalysts in $CH_4$ results in the formation of higher amounts of carbon deposition. Finally, we should consider that the lower $H_2$ observed could also point out a higher participation of coke hydrogenolysis reaction [40].

On this basis, it is clear that reduction pre-treatment at different temperatures strongly conditions the catalytic behavior of Mo/HZSM-5 catalyst. The 550 ºC reduction pre-treatment plainly has a different effect on the catalyst performance, which is reflected in a higher conversion, selectivity and production to aromatics. In addition, this catalyst produces a smaller amount of $H_2$ and coke than the other pre-treated catalysts as well as much smaller than the non-treated 4%Mo/HZSM-5 catalyst. This fact would do have a positive effect on the catalyst stability for *MDA* reaction.

### 3.2. Structural and morphological study of catalysts

In order to understand how the catalyst pre-reduction affects to the final catalytic performance we have studied the structural, morphological and chemical state of catalyst.

By observing the XRD patterns, different reduction treatments do not affect to the crystalline structure of ZSM-5 (Fig. 4). However, the surface features seem to be certainly affected by different reduction pre-treatments (Table 1).

Reduction at lower temperatures shows a slight diminution in BET surface area, mainly affecting to the mesopore fraction (Table 1). On the other side, after reduction at 650 ºC a notable decrease is observed. Therefore, this feature could not be correlated with the lower catalytic performance discussed before. By comparing the not pre-treated spent catalyst with those from pre-reduced series, it is worthy to note that pre-reduction at 550 ºC and 650 ºC clearly induces a significant stress to the surface area, with outstanding diminution of the mesopore fraction, leaving the micropore fraction almost unaffected by the pre-treatment.

After observing the samples by TEM and STEM (Fig. 5), the formation of large agglomerates of molybdenum in the spent 450 ºC pre-treated sample is striking. While a in a previous work $MoO_3$ particles were clearly detected in the Mo10% sample, no peaks of $MoO_3$ appear on XRD [35].

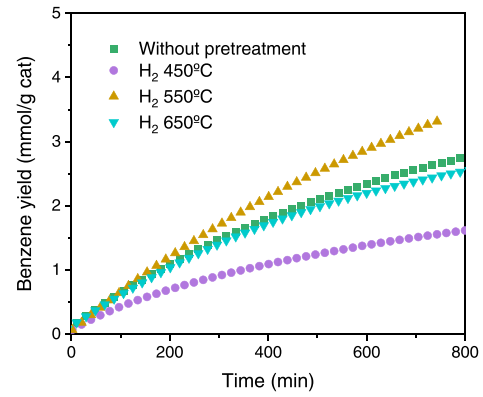


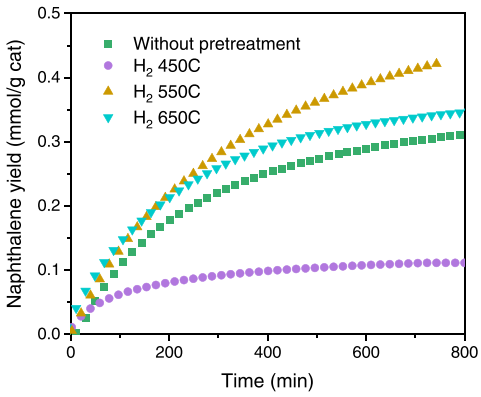


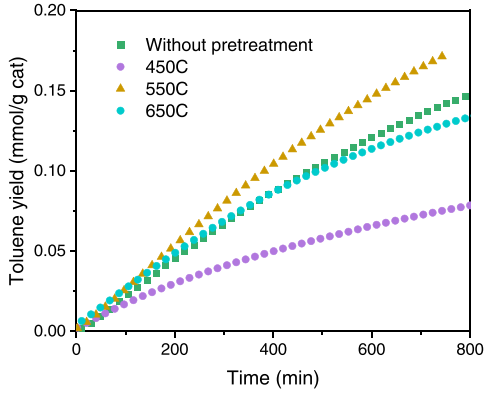


| Sample | Products yield (µmol/$g_{cat}$) @12h | | | Benzene |
|---|---|---|---|---|
| | Benzene | Toluene | Naphthalene | distribution |
| NP | 2.67 | 0.14 | 0.31 | 86% |
| 450°C | 1.57 | 0.08 | 0.11 | 89% |
| 550°C | 3.31 | 0.17 | 0.42 | 85% |
| 650°C | 2.47 | 0.13 | 0.34 | 84% |

**Fig. 2.** Aromatic products yields for 4%Mo/HZSM-5 catalysts during methane dehydroaromatization reaction.

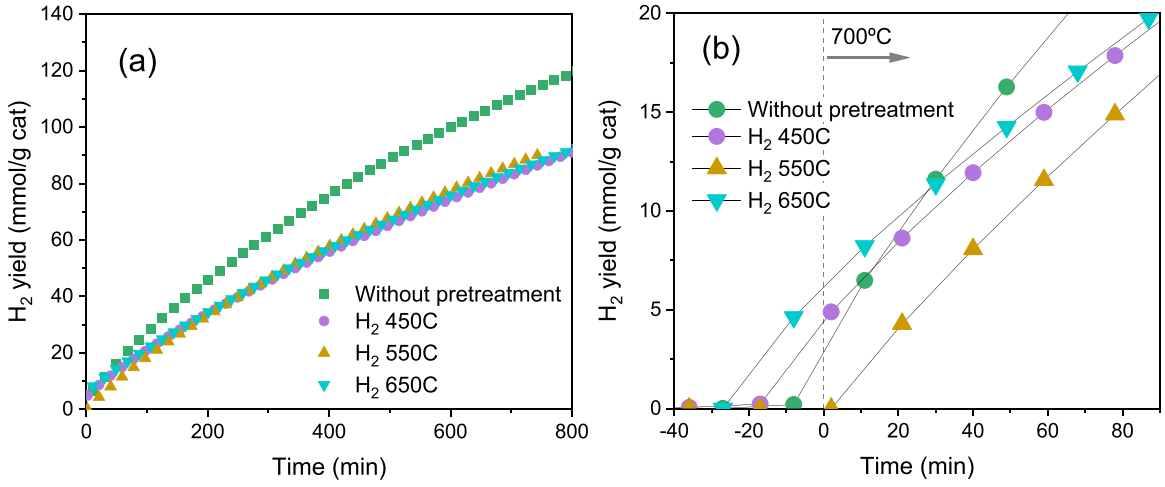


**Fig. 3.** a) $H_2$ yield for Mo/HZSM-5 catalysts during methane dehydroaromatization reaction; b) Detailed $H_2$ evolution at the first stage of reaction.

So, it would indicate that the particles formed are not crystalline. Moreover, the micrographies showed the formation of ca. 50 nm molybdenum agglomerates composed by smaller particles and slightly Al-enriched.

The images obtained for the fresh 4%Mo/HZSM-5 were shown in our previous work [10], and in addition to the homogeneously distributed Mo species, the presence of larger Mo particles associated with Al-enriched areas of the zeolite were detected. However, these particles were usually located on the edge of the zeolite, and the size was around 10 nm and more asymmetric. The agglomeration observed after reaction for 450 ºC pre-reduced catalyst were circular, and the smaller particles inside the agglomeration can be distinguish.

The formation of such evident agglomerated Al-enriched Mo species could be explained by considering that upon reduction step, structural water is evolved from the zeolite. Thus, due to the thermodynamic limitation of water elimination at 450 ºC, slow evolution during isothermal reduction process at 450 ºC, would lead a slow diffusion inside the pore structure.

During this partial dehydration process Al and Mo would be partially segregated forming these large aggregates. Indeed, by observing the mass 18 in the mass spectrometer during TPR experiments after different pre-reduction processes, it is evident that for 450 ºC water evolves outstandingly with respect to pre-reduced at higher temperatures. This fact clearly denotes that at this pre-reduction temperature, structural water would remain in the pore structure creating a certain '*hydrothermal*' ambient (Fig. S3). At such conditions, Al extraction and Mo

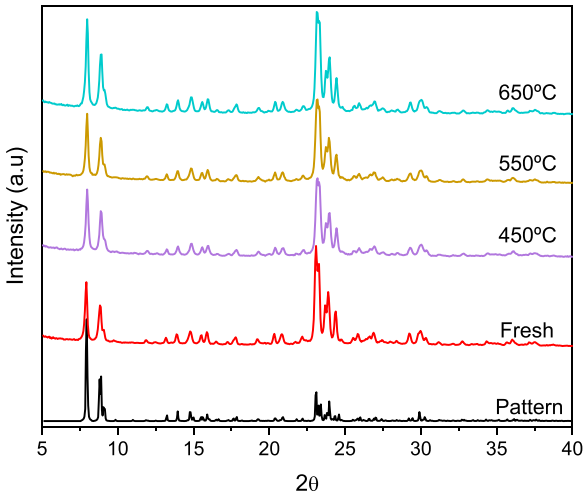


**Fig. 4.** XRD patterns for 4%Mo/HZSM-5 catalysts after different pre-reduction treatment.

**Table 1**
Surface area of fresh, pre-treated and post-reaction catalysts.

| Treatment | T (°C) | Surface area ($m^2/g$) | | $V_{pore}$ ($cm^3/g$) | |
|---|---|---|---|---|---|
| | | BET | micro | Total | Micro |
| Fresh | – | 313 | 236 | 0.17 | 0.11 |
| After 2 h $CH_4$ 700 °C (without pre-treatment) | – | 245 | 207 | 0.14 | 0.10 |
| After 1 h $H_2$ (T) | 450 | 298 | 230 | 0.17 | 0.11 |
| | 550 | 296 | 229 | 0.16 | 0.11 |
| | 650 | 242 | 193 | 0.14 | 0.09 |
| After 1 h $H_2$ (T) and 2 h $CH_4$ 700 °C | 450 | 263 | 220 | 0.14 | 0.10 |
| | 550 | 227 | 199 | 0.12 | 0.09 |
| | 650 | 218 | 202 | 0.11 | 0.09 |

aggregation would be favored forming the observed Al-enriched Mo-aggregates.

For the spent samples pre-reduced at 550 ºC and 650 ºC, these particles are not observed. On the contrary, molybdenum particles seem to be more dispersed, as can observed in Figs. S4-S6. For the 550 ºC pre-reduced catalyst molybdenum particles appear homogeneous in shape and size, with a diameter of 2–4 nm. It is more difficult to resolve the morphology of the particles in spent 650 ºC pre-reduced catalyst. However, it is interesting how in both later samples the formation of carbon nanotubes can be observed. As was explained before, the pre-reduction treatment at 550 ºC and 650 ºC gives rise to a higher conversion to aromatics than pre-reduction treatment at 450 ºC. The formation of these large amorphous Mo-Al agglomerates could be the reason for a smaller conversion and selectivity to aromatics [41].

In addition, the HAADF-STEM images of the spent 4%Mo/HZSM-5 catalyst after the 650 ºC pre-reduction treatment it can be detected some Al-enriched areas. However, unlike in the case of 450 ºC pre-treated catalyst, within these areas molybdenum did not appear aggregated, remaining homogeneously dispersed.

### 3.3. Mo chemical features and surface study

The reducibility of the calcined systems has been followed by temperature programmed reduction measurements. As we have shown in previous works, 4%Mo/HZSM-5 catalyst showed a complex TPR profile, with the presence of at least five different Mo phases, with different location, dispersion and catalytic performances in the *MDA* [42]. In this case, two successive TPR-$H_2$ have been carried out, the first up to 450 ºC, 550 ºC or 650 °C for 1 h, that would be equivalent to the pre-reduction treatment carried out on the samples (Fig. 6**.a**); and the second from 250 ºC to 1000 °C that could help to assess the situation of the catalyst after reduction pre-treatment (Fig. 6**.b**). By comparing with the TPR profile of pre-reduced samples with previous one (Fig. 6**.a**), we have to highlight that reduction pre-treatment induces important modifications in the Mo-species identified in our previous study (Fig. 6**.b**) [42].

The first important issue that might be highlighted is that upon pre-reduction treatment, the Mo species reducing between 350 and 570 °C (*A* Mo-species, ascribed as small clusters of well-dispersed Mo monomers, located on the external surface of the zeolite) disappear almost completely. Furthermore, the reduction regions at 570–680 °C (*B* family, small well-dispersed Mo dimers/polymers clusters, associated with Al-enriched areas of the zeolite) and 680–800 °C (*C* family small well-dispersed Mo dimers/polymers clusters located in the inner micropores) gradually decrease with the pre-reduction treatment temperature, indicating that they are already reduced during pre-treatment.

It should be remembered that the Mo-species reducing at 680–800 °C, were identified as the highly active species for the reaction [42]. On this basis, it could be expected that pre-reduction would progressively improve the catalytic performance as reduction temperature increases. However, as already pointed out, water evolution during reduction pre-treatment appears at ca. 250–300 °C and ends at 600 °C. We have shown that reduction at 450 ºC contributes to the extraction of molybdenum and aluminum to the surface, which under reaction

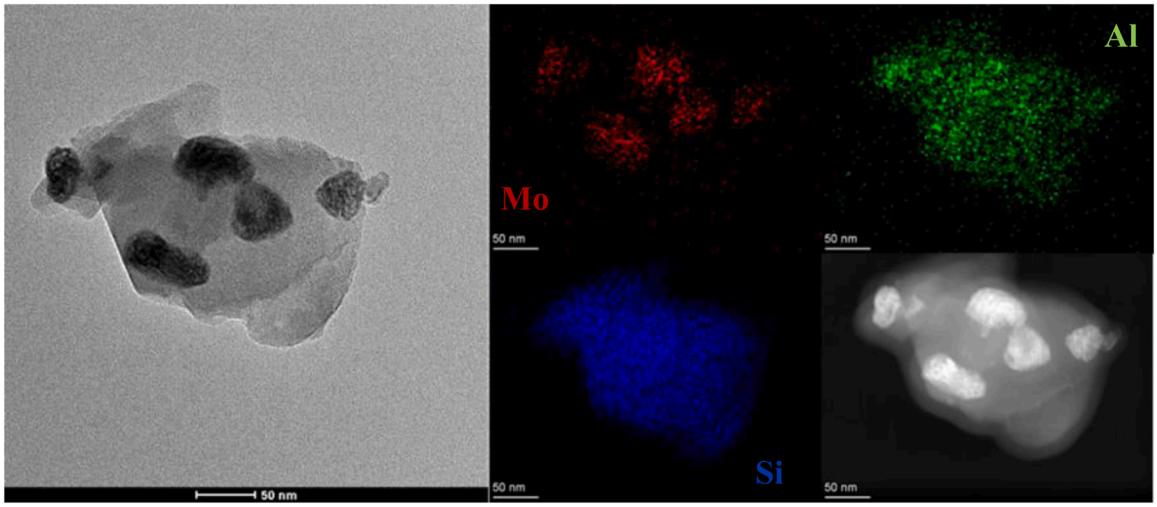


**Fig. 5.** HAADF-STEM images of the spent 4%Mo/HZSM-5 catalyst after the 450 ºC $H_2$ pre-reduction treatment.

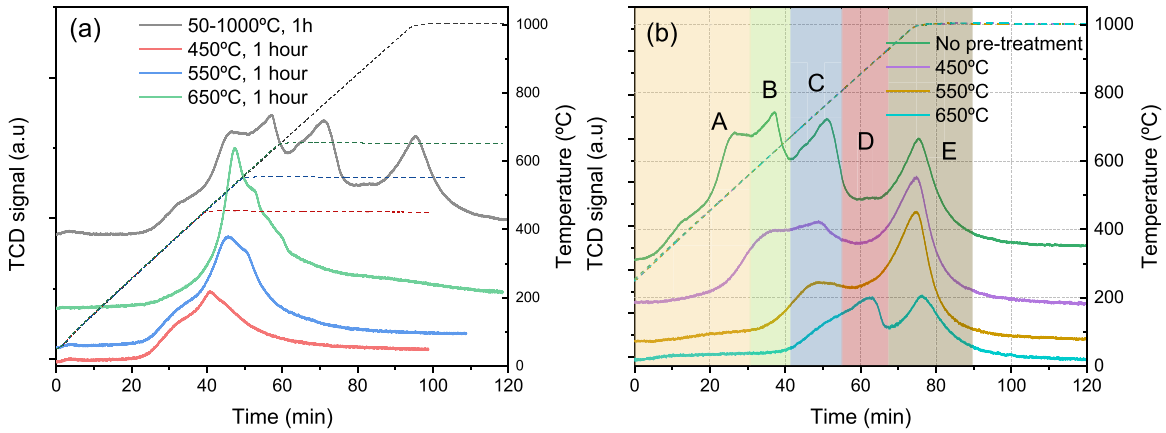


**Fig. 6.** TPR profiles for 4%Mo/HZSM-5 catalysts: a) Reduction pre-treatment profile; b) Reduction profile for pre-reduced catalysts (Letters indicate the identified species from Ref 42).

conditions would agglomerate, forming the particles observed by TEM and HAADF. This leads to a strong decrease in the catalytic activity of the catalyst. On the other hand, pre-reduction at 650 ºC would affect importantly to the surface and structural features of the support. Even more, we have denoted certain surface Al clustering from STEM images. Therefore, in spite of the presence of a higher fraction of Mo-reduced species, such structural and surface detrimental features would lead to a lower catalytic performance. In addition, the catalytic promoting effect of a larger amount of reduced species *C* at 650 ºC pre-reduced catalyst could be reduced by a smaller amount of species *E* (small well-dispersed Mo monomers clusters, that reduce at temperatures higher than 915 °C and located in the inner microporous channels of the zeolite*)*.

As reported in the literature, a reduction treatment of Mo catalyst in $H_2$ flow resulted in an improvement on the stability [43]. However, it is necessary to add that there is an optimal temperature at which to reduce the catalyst in order to obtain a better performance. In this sense, previous studies reported in the literature considers the pre-reduction treatment at the reaction temperature [22,34,43]. As we have demonstrated here, the different reduction temperatures could lead to agglomeration (low conversion and rapid deactivation) or surface/structure deterioration that would adversely affect the catalytic performance and increase at the same time the selectivity to naphthalene.

The study of the physicochemical state of the external surface region is crucial to determine how different reduction pre-treatment could tune the surface Mo-species. Thus, in Fig. 7 we plot the recorded signals of the Mo *3d* and C *1s* regions of the different reduction pre-treatment and after 2 h of reaction.

By observing the Mo *3d* signals of different spent catalysts it is evident the important influence of reduction pre-treatment in the final situation of Mo species. Even more, the chemical composition of the surface seems to be also strongly conditioned by the pre-treatment temperature (Fig. S7). Indeed, the suggested aggregation is plainly observed from the higher Mo/Si ratio obtained for this catalyst with respect to the rest of pre-treated catalysts (Fig. S7). We have to say the for all pre-treated catalysts, the Mo/Si ratios observed are always below the attained one for non pre-treated catalyst. This could indicate that the pre-reduction would induce both, a certain agglomeration of Mo-species or a diffusion inside the zeolite pores. In this sense, there is certain consensus in the fact that the Mo active species are most likely located inside the pores of zeolite [44]. On the contrary, Mo-carbide at the outer zeolite surface seems to grow further and has been related to the primary cause of catalyst deactivation [45]. Additionally, the Al/Si ratio also suffers a particular variation depending on the reduction temperature, being slightly lower in the case of the catalyst pre-reduced at 550 ºC. In fact, we have demonstrated from HAADF mapping images clear Al

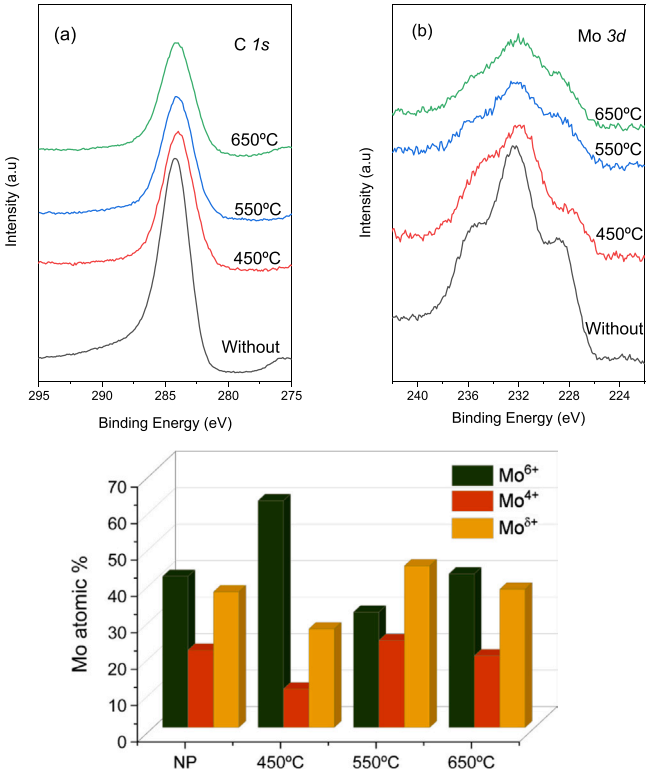


**Fig. 7.** *Upper panel*: a) Normalized Mo *3d* and b) C *1s* spectra of the spent 4% Mo/HZSM-5 catalysts with and without reduction pre-treatment. *Lower panel*: Atomic % for different Mo oxidation states from Mo *3d* deconvolution.

aggregation after pre-reduction at 450 ºC and 650 ºC.

Moreover, by deconvoluting the Mo *3d* spectra (Fig. S8) we have found interesting differences in the Mo chemical state after different processes (Fig. 7, *lower panel*). Thus, it is worthy to mention the high fraction of $Mo^{6+}$ found in the catalyst pre-reduced at 450 ºC. The occurrence of this oxidized species could be correlated with the observed Mo extraction/aggregation due to the important water evolution during reduction pre-treatment. Similarly, but at less extent, the pre-reduction at 650 ºC also favors the presence of $Mo^{6+}$. On the contrary, $Mo^{\delta+}$ species appear prominently in the catalyst pre-reduced at 550 ºC. Another important issue concerns to the C *1s* signal (Fig. 7). In all pre-reduced catalysts, the surface carbon content appears significantly lower confirming the observation from DTG analysis of spent samples.

From these results, we may argue that pre-reduction at different

temperatures induces particular effects on surface Mo that could strongly condition the final catalytic performance. In this sense, the more active catalysts, obtained after pre-reduction at 550 ºC, shows a higher fraction of $Mo^{\delta+}$ with a lower fraction of Al. On the contrary, reduction pre-treatment at 450 ºC or 650 ºC would favor $Mo^{6+}$ and/or Al extraction.

## 4. Conclusions

The results showed that a reduction pre-treatment with $H_2$ could help to improve the catalytic performance of Mo/HZSM-5 on *MDA* reaction. Moreover, we have shown that the temperature at which the reduction is carried out has a strong influence on both, the position and the state of the molybdenum species.

Thus, from TPR experiments and STEM images we have shown that reduction of the samples revealed that the pre-treatment of hydrogen at different temperatures causes the redistribution of molybdenum species in the zeolite. Such reorganization was corroborated from XPS analysis. A clear correlation between the amount of $Mo^{\delta+}$ species and the catalytic performance (conversion and selectivity to aromatics) on the 4% Mo/HZSM-5 catalysts was proved.

Optimum catalyst performance was attained for the sample subjected to a pre-treatment at 550 °C which showed great improvements in catalytic activity over the catalyst without pre-treatment and pre-treated at 450 ºC and 650 ºC. The fact that the total methane conversion was lower contributed to the lower obtainment of coke in the sample after pre-treatment. The greater selectivity to aromatics and the greater formation of these could be due to the greater degree of reduction of the alkalized surface molybdenum species in the sample reduced to this temperature, and to the fact that the molybdenum seems to be found inside the structure, whereby it can be detected by TPR but not by XPS.

It has been evidenced that the complex evolution of Mo species observed upon reduction pre-treatment is closely related to the support feature. Therefore, it would be interesting to consider other zeolite supports such as MCM-22 with different pore structuration in order to achieve better catalytic performance and catalyst stability.

## CRediT authorship contribution statement

**A. López-Martín:** Methodology, Investigation, Writing-Original draft preparation. **G. Colón:** Conceptualization, Methodology, Writing-Original draft preparation, Writing-Reviewing and Editing, Supervision. **A. Caballero:** Conceptualization, Methodology, Supervision.

## Declaration of Competing Interest

The authors declare that they have no known competing financial interests or personal relationships that could have appeared to influence the work reported in this paper.

## Acknowledgments

Authors acknowledge the financial support through grants ENE2017-88818-C2-1-R and PID2020-119946RB-I00 funded by spanish MCIN/AEI/ 10.13039/501100011033 and, as appropriate, by “ERDF A way of making Europe”, by the “European Union NextGenerationEU/PRTR”.

## Appendix A. Supporting information

Supplementary data associated with this article can be found in the online version at doi:10.1016/j.apcatb.2022.121382.

## References

[1] W. Taifan, J. Baltrusaitis, $CH_4$ conversion to value added products: potential, limitations and extensions of a single step heterogeneous catalysis, Appl. Catal. B Environ. 198 (2016) 525–547.
[2] L. He, Y. Fan, J. Bellettre, J. Yue, L. Luo, A review on catalytic methane combustion at low temperatures: Catalysts, mechanisms, reaction conditions and reactor designs, Renew. Sustain. Energy Rev. 119 (2020), 109589.
[3] J.J. Spivey, G. Hutchings, Catalytic aromatization of methane, Chem. Soc. Rev. 43 (2014) 792–803.
[4] K. Jawaharraj, N. Shrestha, G. Chilkoor, S.S. Dhiman, J. Islam, V. Gadhamshetty, Valorization of methane from environmental engineering applications: a critical review, Water Res. 18715 (2020), 116400.
[5] J. Bao, G. Yang, Y. Yoneyama, N. Tsubaki, Significant advances in C1 catalysis: highly efficient catalysts and catalytic reactions, ACS Catal. 9 (2019) 3026–30535.
[6] L. Sun, Y. Wang, N. Guan, L. Li, Methane activation and utilization: current status and future challenges, Energy Technol. 8 (2020) 1900826.
[7] P. Schwach, X. Pan, X. Bao, Direct conversion of methane to value-added chemicals over heterogeneous catalysts: challenges and prospects, Chem. Rev. 117 (2017) 8497–8520.
[8] T. Zhang, Recent advances in heterogeneous catalysis for the nonoxidative conversion of methane, Chem. Sci. 12 (2021) 12529–12545.
[9] S.V. Konnov, Direct non-oxidative conversion of methane over metal-containing zeolites: main strategies for shifting the thermodynamic equilibrium, Pet. Chem. (2022).
[10] A. Galadima, O. Muraza, Advances in catalyst design for the conversion of methane to aromatics: a critical review, Catal. Surv. Asia 23 (2019) 149–170.
[11] D. Kiani, S. Sourav, Y. Tang, J. Baltrusaitis, I.E. Wachs, Methane activation by ZSM-5-supported transition metal centers, Chem. Soc. Rev. 50 (2021) 1251–1268.
[12] S. Kasipandi, J.W. Bae, Recent advances in direct synthesis of value-added aromatic chemicals from syngas by cascade reactions over bifunctional catalysts, Adv. Mater. 31 (2019) 1803390.
[13] N. Kosinov, E.J.M. Hensen, Reactivity, selectivity, and stability of zeolite-based catalysts for methane dehydroaromatization, Adv. Mater. 32 (2020) 2002565.
[14] C. Brady, Q. Debruyne, A. Majumder, B. Goodfellow, R. Lobo, T. Calverley, B. Xu, An integrated methane dehydroaromatization and chemical looping process, Chem. Eng. J. 406 (2021), 127168.
[15] N. Wang, X. Dong, L. Liu, D. Cai, Q. Cheng, J. Wang, Y. Hou, A.H. Emwas, J. Gascon, Y. Han, Probing the catalytic active sites of Mo/HZSM-5 and their deactivation during methane dehydroaromatization, Cell Rep. Phys. Sci. 2 (2021), 100309.
[16] I. Vollmer, I. Yarulina, F. Kapteijn, J. Gascón, Progress in developing a structure-activity relationship for the direct aromatization of methane, ChemCatChem 11 (2019) 39–52.
[17] B.J. Lee, Y.G. Hur, D.H. Kim, S.H. Lee, K.Y. Lee, Non-oxidative aromatization and ethylene formation over Ga/HZSM-5 catalysts using a mixed feed of methane and ethane, Fuel 253 (2019) 449–459.
[18] C.H. Tempelman, E.J. Hensen, On the deactivation of Mo/HZSM-5 in the methane dehydroaromatization reaction, Appl. Catal. B: Environ 177–176 (2015) 731–739.
[19] Y. Song, Q. Zhang, Y. Xu, Y. Zhang, K. Matsuoka, Z.G. Zhang, Coke accumulation and deactivation behavior of microzeolite-based Mo/HZSM-5 in the non-oxidative methane aromatization under cyclic $CH_4$-$H_2$ feed switch mode, Appl. Catal. A Gen. 530 (2017) 12–20.
[20] I. Julian, J.L. Hueso, N. Lara, A. Solé-Daurá, J.M. Poblet, S.G. Mitchell, R. Mallada, J. Santamaría, Polyoxometalates as alternative Mo precursors for methane dehydroaromatization on Mo/ZSM-5 and Mo/MCM-22 catalysts, Catal. Sci. Technol. 9 (2019) 5927–5942.
[21] V. Abdelsayed, D. Shekhawat, M.W. Smith, Effect of Fe and Zn promoters on Mo/HZSM-5 catalyst for methane dehydroaromatization, Fuel 139 (2015) 401–410.
[22] A. Sridhar, M. Rahman, S.J. Khatib, Enhancement of molybdenum/ZSM-5 catalysts in methane aromatization by the addition of iron promoters and by reduction/carburization pretreatment, ChemCatChem 10 (2018) 2571–2583.
[23] D. Kiani, S. Sourav, J. Baltrusaitis, I.E. Wachs, Oxidative coupling of methane (OCM) by $SiO_2$-supported tungsten oxide catalysts promoted with Mn and Na, ACS Catal. 9 (2019) 5912–5928.
[24] A. Sridhar, M. Rahman, A. Infantes-Molina, B.J. Wylie, C.G. Borcik, S.J. Khatib, Bimetallic Mo-Co/ZSM-5 and Mo-Ni/ZSM-5 catalysts for methane dehydroaromatization: a study of the effect of pretreatment and metal loadings on the catalytic behavior, Appl. Catal. A Gen. 589 (2020), 117247.
[25] A. López-Martín, M.F. Sini, M.G. Cutrufello, A. Caballero, G. Colón, Characterization of Re-Mo/ZSM-5 catalysts: How Re improves the performance of Mo in the methane dehydroaromatization reaction, Appl. Catal. B Environ. 304 (2022), 120960.
[26] M.A. Abedin, S. Kanitkar, S. Bhattar, J.J. Spivey, Methane dehydroaromatization using Mo supported on sulfated zirconia catalyst: effect of promoters, Catal. Today 365 (2021) 71–791.
[27] P. Tang, Q. Zhu, Z. Wu, D. Ma, Methane activation: the past and future, Energy Environ. Sci. 7 (2014) 2580–2591.
[28] K. Sun, D.M. Ginosar, T. He, Y. Zhang, M. Fan, R. Chen, Progress in nonoxidative dehydroaromatization of methane in the last 6 years, Ind. Eng. Chem. Res. 57 (2018) 1768–1789.
[29] C.H.L. Tempelman, E.J.M. Hensen, On the deactivation of Mo/HZSM-5 in the methane dehydroaromatization reaction, Appl. Catal. B Environ. 176 – 177 (2015) 731–739.
[30] C.H.L. Tempelman, X.C. Zhu, E.J.M. Hensen, Activation of Mo/HZSM-5 for methane aromatization, Chin. J. Catal. 36 (2015) 829–837.

[31] M.T. Portilla, F.J. Llopis, M. Moliner, C. Martinez, Influence of preparation conditions on the catalytic performance of Mo/H-ZSM-5 for methane dehydroaromatization, Appl. Sci. 11 (2021) 5465.
[32] M.T. Portilla, F.J. Llopis, C. Martínez, Non-oxidative dehydroaromatization of methane: an effective reaction-regeneration cyclic operation for catalyst life extension, Catal. Sci. Technol. 5 (2015) 3806–38211.
[33] I. Vollmer, B. van der Linden, S. Ould-Chikh, A. Aguilar-Tapia, I. Yarulina, E. Abou-Hamad, Y.G. Sneider, A.I. Olivos Suarez, J.L. Hazemann, F. Kapteijn, J. Gascon, On the dynamic nature of Mo sites for methane dehydroaromatization, Chem. Sci. 9 (2018) 4801–4807.
[34] M. Rahman, A. Sridhar, S.J. Khatib, Impact of the presence of Mo carbide species prepared ex situ in Mo/HZSM-5 on the catalytic properties in methane aromatization, Appl. Catal. A Gen. 558 (2018) 67–80.
[35] A. López-Martín, A. Caballero, G. Colón, Structural and surface considerations on Mo/ZSM-5 systems for methane dehydroaromatization reaction, Mol. Catal. 486 (2020), 110787.
[36] U. Menon, M. Rahman, S.J. Khatib, A critical literature review of the advances in methane dehydroaromatization over multifunctional metal-promoted zeolite catalysts, Appl. Catal. A Gen. 608 (2020), 117870.
[37] Y. Gu, P. Chen, H. Yan, X. Wang, Y. Lyu, Y. Tian, W. Liu, Z. Yan, X. Liu, Coking mechanism of Mo/ZSM-5 catalyst in methane dehydroaromatization, Appl. Catal. A: Gen. 613 (2021), 118019.
[38] I. Vollmer, S. Ould-Chikh, A. Aguilar-Tapia, G. Li, E. Pidko, J.L. Hazemann, F. Kapteijn, J. Gascón, Activity descriptors derived from comparison of Mo and Fe as active metal for methane conversion to aromatics, J. Am. Chem. Soc. 141 (2019) 18814–18824.
[39] G. Li, I. Vollmer, C. Liu, J. Gascon, E.A. Pidko, Relevance of the Mo-precursor state in H-ZSM-5 for methane dehydroaromatization, ACS Catal. 9 (2019) 8731–8737.
[40] A. Samanta, X. Bai, B. Robinson, H. Chen, J. Hu, Conversion of light alkane to value-added chemicals over ZSM-5/metal promoted catalysts, Ind. Eng. Chem. Res. 56 (2017) 11006–11012.
[41] A. Sridhar, M. Rahman, A. Infantes-Molina, B.J. Wylie, C.G. Borcik, S.J. Khatib, Bimetallic Mo-Co/ZSM-5 and Mo-Ni/ZSM-5 catalysts for methane dehydroaromatization: a study of the effect of pretreatment and metal loadings on the catalytic behavior, Appl. Catal. A Gen. 589 (2020), 117247.
[42] A. López-Martín, F. Platero, G. Colón, A. Caballero, Elucidating the nature of Mo species on ZSM-5 and its role in the methane aromatization reaction, React. Chem. Eng. 6 (2021) 1265–1276.
[43] M. Rahman, A. Infantes-Molina, A. Boubnov, S.R. Bare, E. Stavitski, A. Sridhar, S. J. Khatib, Increasing the catalytic stability by optimizing the formation of zeolite-supported Mo carbide species ex situ for methane dehydroaromatization, J. Catal. 375 (2019) 314–328.
[44] N. Kosinov, F.J.A.G. Coumans, E.A. Uslamin, A.S.G. Wijpkema, B. Mezari, E.J. M. Hensen, Methane dehydroaromatization by Mo/HZSM-5: mono- or bifunctional catalysis? ACS Catal. 7 (2017) 520–529.
[45] N. Kosinov, E.A. Uslamin, L. Meng, A. Parastaev, Y. Liu, E.J.M. Hensen, Reversible nature of coke formation on Mo/ZSM-5 methane dehydroaromatization, Catal. Angew. Chem. Int. Ed. 58 (2019) 7068–7072.